

## Research Article

# Analytical Design and Optimization of an Automotive Rubber Bushing

Jonathan Rivas-Torres,<sup>1</sup> Juan C. Tudon-Martinez ,<sup>1</sup> Jorge de-J. Lozoya-Santos,<sup>2</sup> Ricardo A. Ramirez-Mendoza,<sup>2</sup> and Andrea Spaggiari <sup>3</sup>

<sup>1</sup>Universidad de Monterrey, Ignacio Morones Prieto 4500, Jesús M. Garza, 66238 San Pedro Garza García, NL, Mexico

<sup>2</sup>Tecnológico de Monterrey, Av. E. Garza Sada, Col. Tecnológico, 64849 Monterrey, NL, Mexico

<sup>3</sup>Università degli Studi di Modena e Reggio Emilia, Via Giovanni Amendola, 2, 42122 Reggio Emilia, Italy

Correspondence should be addressed to Juan C. Tudon-Martinez; [juan.tudon@udem.edu](mailto:juan.tudon@udem.edu)

Received 6 November 2018; Revised 3 February 2019; Accepted 20 February 2019; Published 26 March 2019

Academic Editor: Jussi Sopanen

Copyright © 2019 Jonathan Rivas-Torres et al. This is an open access article distributed under the Creative Commons Attribution License, which permits unrestricted use, distribution, and reproduction in any medium, provided the original work is properly cited.

The ride comfort, driving safety, and handling of the vehicle should be designed and tuned to achieve the expectations defined in the company's design. The ideal method of tuning the characteristics of the vehicle is to modify the bushings and mounts used in the chassis system. To deal with the noise, vibration and harshness on automobiles, elastomeric materials in mounts and bushings are determinant in the automotive components design, particularly those related to the suspension system. For most designs, stiffness is a key design parameter. Determination of stiffness is often necessary in order to ensure that excessive forces or deflections do not occur. Many companies use trial and error method to meet the requirements of stiffness curves. Optimization algorithms are an effective solution to this type of design problems. This paper presents a simulation-based methodology to design an automotive bushing with specific characteristic curves. Using an optimum design formulation, a mathematical model is proposed to design and then optimize structural parameters using a genetic algorithm. To validate the resulting data, a finite element analysis (FEA) is carried out with the optimized values. At the end, results between optimization, FEA, and characteristic curves are compared and discussed to establish the correlation among them.

## 1. Introduction

Bushings are used in the automotive industry to improve ride comfort, safety, and handling. With the continued development of chassis dynamics, the ability of the suspension to execute precisely defined movements in response to applied forces has become more important. Chassis dynamics engineers require that suspension components execute precisely specified movements in many different directions. The required force-displacement behaviors lead to increased expectations for the design of the bushings. In order to achieve the current level of noise attenuation, rubber bushings and mounts have been used to solve a number of conflicts between the requirements for vehicle handling and cabin acoustics. The high-frequency characteristics of the rubber-metal components themselves are dependent not only on the properties of the materials but

also on the geometries and assembly techniques used [1]. During the vehicle development process, optimization of the rubber products is also needed to have target stiffness curves [2]. Design objectives usually include structural weight and cost [3].

Ride comfort and harshness performance of the vehicle can be improved by optimizing the characteristics of the suspension system components [4]. There is some related work that can be found in the literature about optimizing techniques in automotive applications, specifically in suspension components. Kaya [2] performed an optimization of shape of a rubber bushing using a Pascal code based on the differential evolution algorithm. This method is particularly suited where there is no relationship between the objective function and the design variables. Kaldas et al. [4] developed an optimization technique to improve vehicle ride comfort and harshness using a genetic algorithm to determine the

optimum damper top mount characteristics. Li et al. [5] performed a genetic algorithm to find the optimal coordinates of hard points, which are the key locations to influence on suspension characteristics depending on their relative orientations, on a double-wishbone type suspension system. Mitra et al. [6] used factorial methods of design of experiments to optimize a suspension performance in a quarter car test rig. Three and six suspension parameters were optimized and compared with experimental data obtaining high correlation. Zhou et al. [7] optimized the basic parameters of a double suspension arm torsion bar for decreasing displacement of the suspension and limiting the frequency of impacting the stop block using a nonlinear multitarget optimizing tool box from MATLAB. Pang et al. [8] carried out a ride comfort optimization of a heavy vehicle's suspension based on Adams, using a sequential quadratic programming method. Xu et al. [9], based on the genetic algorithm and the fusion robustness analysis, performed an optimization of the stiffness of a powertrain mounting system in 6 DOF. Tikani et al. [10] proposed a new hydraulic engine mount with controllable inertia track profile. Optimum values of rubber length and diameter for a typical 4-cylinder car were obtained with a genetic optimization algorithm. Özcan et al. [11] performed an SQP optimization using MATLAB to find the optimum spring and damper characteristics of a quarter and a half of a vehicle model.

All aforementioned papers stress the necessity of optimizing the design of the automotive suspension components. More focused on rubber bushing design, some authors [2, 18, 19] have proposed the use of the finite element analysis (FEA) software; in this case, complex structural simulations support the design by analyzing the behavior of the stresses and strains in multiple directions. FEA allows bushing designs to be constructed, refined, and optimized before the design is manufactured; however, the analysis can cost more due to the requirement of more computational resources, specialized software licenses, and too much time design due to the processing time. On the contrary, a multidisciplinary design optimization such as a multiobjective optimization approach is an attractive solution to optimize the bushing design problem by relaxing the computational effort; multiple objective functions with proper constraints in a formal mathematical formulation allows focusing the optimal design in particular features, not only technical, but also economical.

In this paper, a multiobjective optimization problem has been proposed to design an automotive suspension rubber bushing, considering the multiple objectives as the desired stiffness characteristics curves. In this sense, the rubber bushing design is based on the desired radial, axial, and torsional stiffness property. Based on multiple optimization problem formulation, a mathematical model is defined to design and then optimize structural parameters using a goal attainment algorithm in the Optimization Toolbox™ of MATLAB®. The obtained results are validated with an FEA-based simulation such that the proposed methodology ensures the optimal parameters of rubber bushing.

This paper is organized as follows: a brief introduction to the automotive bushings is presented in the next section.

Section 3 describes the generalities of an optimization problem, while Section 4 presents a five-step methodology used for an optimum design formulation of an automotive bushing based on the problem of ride comfort, handling, and vehicle safety; the problem was translated to a well-defined mathematical statement, whose solution algorithm is detailed in Section 5. Finally, the design results for an automotive rubber bushing with specific stiffness for vehicle quality ride and handling are presented in Section 6. Section 7 concludes the paper.

## 2. Automotive Bushings

A bushing is typically composed of a hollow elastomer cylinder contained between inner and outer cylindrical steel sleeves [12]. This attachment joins components between the suspension system and allows the oscillations and vibrations in the metal component to be transferred to the rubber, where they are damped or eliminated [1, 26]; thus, rubber is an engineering material. To design adequately a rubber, basic mechanical properties must be appreciated [13]. During normal use, the bushing sleeves undergo displacements and rotations relative to one another about axes both along and perpendicular to the centerline of the sleeves. The most important modes of deformation in an automotive suspension, which are the ones studied in this work, include radial, torsional, and axial deformations (Figure 1). The radial mode is defined as a translation perpendicular to the centerline of one sleeve relative to the other fixed sleeve. The torsional and axial modes are defined as rotation and translation of one sleeve relative to the other sleeve about and through the centerline, respectively. In the torsional deflection, the outer sleeve is fixed and rotating the inner sleeve such that a moment/torque is produced in line on the horizontal axis.

Tube form is widely used products as they offer flexibility in torsion, tilt, axial, and radial directions. In the torsion and axial directions, the rubber is used in shear and provides relatively low stiffness. In the radial direction, the rubber is used in compression and tension which provides more stiffness and hence greater stability [13].

In bushing designs, the stiffness is the characteristic of interest to the designer. The units for stiffness or spring rate are Newtons per millimeter (N/mm) for radial and axial directions. For these modes of deflection, in general, the stiffness can be interpreted as the amount of force required to cause a unit of deflection:

$$K = \frac{F}{d}. \quad (1)$$

On the contrary, for the torsional deflection mode, the stiffness  $K_T$  refers to the mechanical capacity of a material of suffering a torsional shearing deformation; in general, it can be defined as the ratio of applied torsion moment to angle of twist with units N·mm/rad, such that

$$K_T = \frac{M}{\theta}. \quad (2)$$

Standard rubber bushings are used to mount chassis and suspension components such as the control arms, dampers,

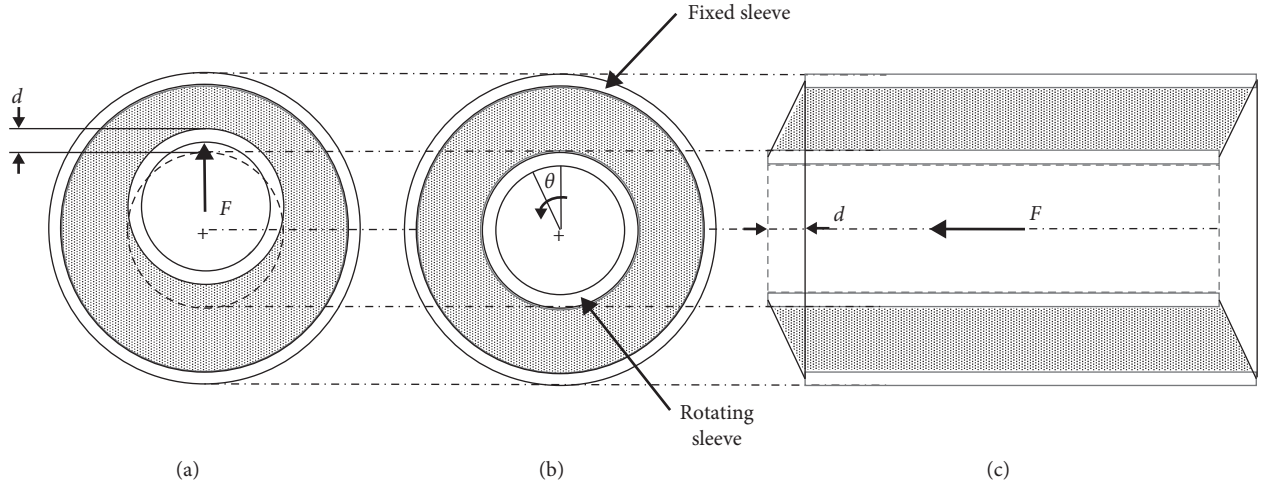


FIGURE 1: Typical modes of deflection in an automotive bushing: (a) radial, (b) torsional, and (c) axial.

and subframes. In Figure 2, the stiffness directions of an automotive bushing in a quarter of a vehicle are showed. The most prevalent force-displacements are presented during cornering, braking, acceleration, road surface irregularities, and wheel imbalances. Depending on the location of the component in the vehicle, the behavior and the directions of the forces can be different.

### 3. Optimization

The design of a system can be formulated as an optimization problem in which a performance measure is minimized/maximized while all other requirements are satisfied. Any problem in which certain parameters need to be determined to satisfy constraints can be formulated as one optimization problem [14].

Optimization is a mathematical technique to find extreme values, without loss of generality, a minimum of a given objective function,  $f(x)$ , subject to some constraints on which coordinates  $x$  are acceptable. Such an optimization problem can be defined as in the following equation:

$$\min_x f(x), \quad (3)$$

such that

$$\begin{aligned} h_i(x) &= 0, \quad i = 1, \dots, m_e, \\ g_i(x) &\leq 0, \quad i = m_e + 1, \dots, m. \end{aligned} \quad (4)$$

A point with the lowest objective value is called an optimizer, and the corresponding objective value is called the optimal value, together they are the optimum. A point is called feasible if it satisfies all the constraints, and the set of all feasible points is called the feasible set or the feasible region [15].

A wide variety of problems in engineering, industry, and many other fields, involve the simultaneous optimization of several objectives. In many cases, the objectives are defined in incomparable units, and they present some degree of conflict among them. These kinds of problems are called Multiobjective Optimization Problems [16].

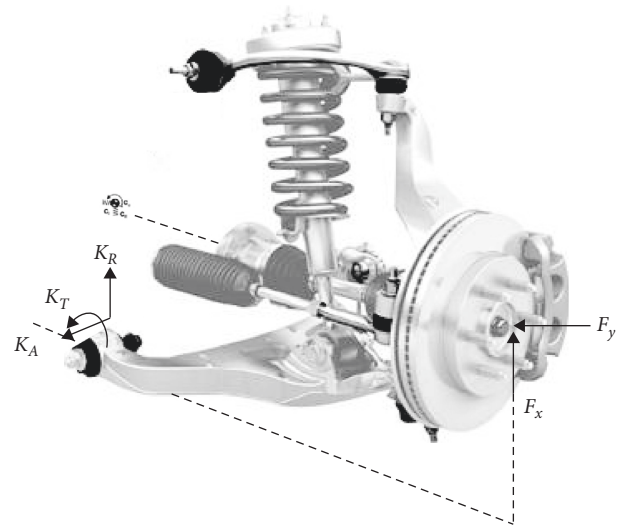


FIGURE 2: Lower control arm bushing with radial, torsional, and axial stiffness directions.

Many numerical methods of optimization have been developed and used to design better systems. It turns out that several commercial computer programs, such as Excel Solver, Mathematica Optimization Toolbox, MATLAB® Optimization Tool Box, and others, are available to solve an optimization problem once it has been properly formulated [14]. The Optimization Toolbox for MATLAB® is the one we use for this study.

**3.1. Multiobjective Optimization Goal Attainment.** Multiobjective optimization involves minimizing or maximizing multiple objective functions subject to a set of constraints. There are two Optimization Toolbox™ in MATLAB® multiobjective solvers: fgoalattain and fminimax. The first one is that we use for this study.

Multiobjective Goal Attainment addresses the problem of reducing a set of nonlinear function  $F_i(x)$  below a set of goal  $F_i^*$ . Since there are several functions  $F_i(x)$ , it is not

always clear what it means to solve this problem, especially when you cannot achieve all the goals simultaneously. Therefore, the problem is reformulated to one that is always well-defined.

The unscaled goal attainment problem is to minimize the maximum of

$$F_i(x) - F_i^*. \quad (5)$$

In this approach, the decision maker must provide a set of design goals  $F^* = \{F_1^*, F_2^*, \dots, F_m^*\}$ , associated with a set of objectives  $F(x) = \{F_1(x), F_2(x), \dots, F_m(x)\}$ . In addition, the decision maker must provide a set of weights  $w = \{w_1, w_2, \dots, w_k\}$  relating the under or overachievement of the desired goals and is expressed as a standard optimization problem using the following formulation [16]:

$$\begin{aligned} &\text{minimize } \Upsilon, \\ &\Upsilon \in \mathbb{R}, x \in \Omega \end{aligned} \quad (6)$$

such that

$$F(x) - w_i \cdot \Upsilon \leq F_i^*, \quad i = 1, \dots, m, \quad (7)$$

where  $\Upsilon$  is a scalar variable unrestricted in sign, and the weights  $\{w_1, w_2, \dots, w_k\}$  are normalized so that

$$\sum_{i=1}^k |w_i| = 1. \quad (8)$$

The term  $w_i \cdot \Upsilon$  introduces an element of slackness into the problem, which otherwise imposes that the goals be rigidly met. The weighting vector,  $w$ , enables the designer to express a measure of the relative tradeoffs between the objectives. For instance, setting the weighting vector  $w$  equal to the initial goals indicates that the same percentage under or overachievement of the goals,  $F^*$ , is achieved. To incorporate hard constraints into the design, a particular weighting factor can be set to zero (i.e.,  $w_i = 0$ ). The goal attainment method provides a convenient intuitive interpretation of the design problem, which is solvable using standard optimization procedures. The method is represented geometrically in Figure 3.

Specification of the goals,  $\{F_1^*, F_2^*\}$ , defines the goal point,  $P$ . The weighting vector defines the direction of search from  $P$  to the feasible function space,  $\Lambda(\Upsilon)$ . During optimization,  $\Upsilon$  is varied, which changes the size of the feasible region. The constraint boundaries converge to the unique solution point  $F_{1s}, F_{2s}$  [17].

In this sense, the fgoalattain algorithm considers  $\Upsilon$  as a slack variable used as a dummy argument to minimize the vector of objectives  $F(x)$  (set of nonlinear functions) in simultaneous way. Generally, prior to optimization, it is unknown whether the objectives will reach the design goals  $F^*$  (under attainment) or is minimized less than the goals (over attainment); to control simultaneously the aforementioned attainment issues on the objectives, the weighting vector over  $\Upsilon$  is considered, such that  $\Upsilon$  makes this multiobjective optimization problem less rigid.

The fgoalattain algorithm uses a Sequential Quadratic Programming (SQP) method to solve iteratively a constrained nonlinear optimization problem. Basically, the SQP

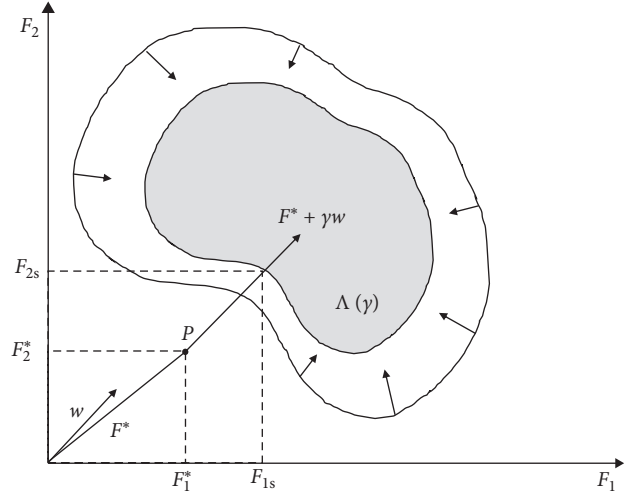


FIGURE 3: Goal attainment method with two objective functions.

method solves a sequence of optimization subproblems; each subproblem optimizes a quadratic model of the objective subject to the linearization of the constraints using a Lagrangian function. Thus, given the nonlinear programming problem,

$$\begin{aligned} &\text{minimize}_{\Upsilon \in \mathbb{R}, x \in \Omega} \quad \Upsilon, \\ &\text{s.t.} \quad b_i(x) : F_i^* - F(x) + w_i \cdot \Upsilon \geq 0, \\ &\quad \sum_{i=1}^k |w_i| = 1. \end{aligned} \quad (9)$$

A QP subproblem based on a quadratic approximation of the Lagrangian function can be formulated as follows:

$$\mathcal{L}(x, \lambda_i) = \Upsilon + \sum_{i=1}^m \lambda_i \cdot b_i(x), \quad (10)$$

where  $\lambda_i$  are the Lagrange multipliers. At any iteration  $x_k$ , the SQP algorithm defines an appropriate search direction  $d_k$  as a solution to the following QP subproblem:

$$\begin{aligned} &\text{minimize}_d \quad \nabla \Upsilon^T d + \frac{1}{2} d^T H_k d, \\ &\text{s.t.} \quad b_i(x_k) + \nabla b_i(x_k)^T d \geq 0, \end{aligned} \quad (11)$$

where  $H_k = \nabla_{xx}^2 \mathcal{L}(x_k, \lambda_{ik})$  is a positive definite approximation of the Hessian matrix of the Lagrangian function.

#### 4. Optimum Design Problem Formulation for an Automotive Bushing

The formulation of an optimum design problem involves translating a descriptive statement of it into a well-defined mathematical statement. It is critical to follow well-defined procedures for formulating design optimization problems. In this section, the next five-step formulation [14] procedure has been considered for the bushing design optimization problem.

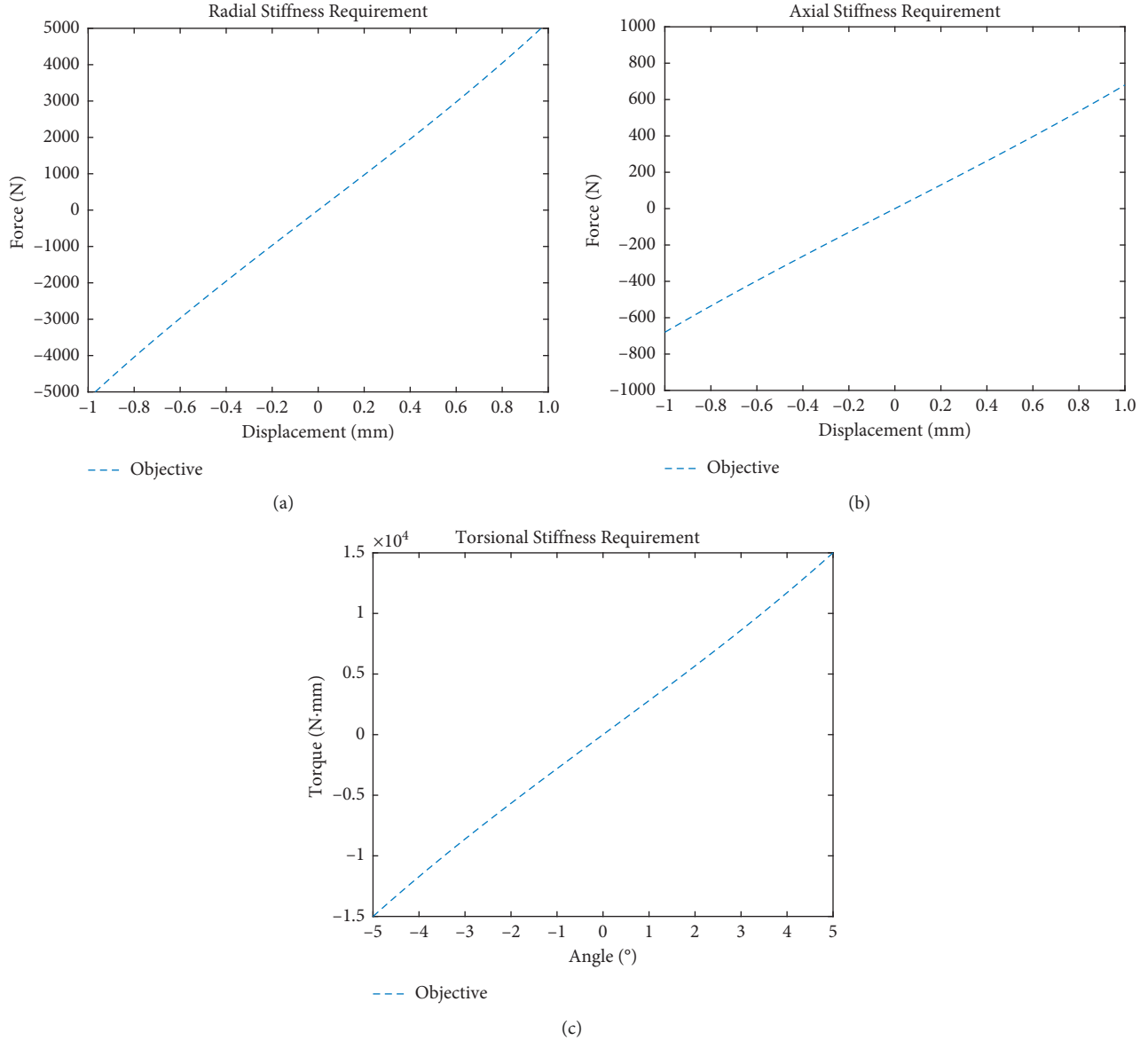


FIGURE 4: Characteristics curves in radial (a), axial (b), and torsional (c).

**4.1. Problem Definition.** For this study, a simple case related to designing a control arm bushing is simulated. The required behavior for the bushing in term of stiffness is formulated based on the problem definition of [18, 19]. Figures 4(a)–4(c) represent typical target characteristic curves of stiffness in (a) radial, (b) axial, and (c) torsional modes to achieve ride comfort, safety, and handling. Usually for a front or rear McPherson suspension mechanism, the axial stiffness is linear between  $\pm 15$  mm of displacement, the torsional is linear between  $\pm 10^\circ$  and, although the radial stiffness is nonlinear in the normal automotive suspension behavior, it can be considered linear for short displacements ( $\pm 1.5$  mm) [28]. The above result supports the linearity considered in the target stiffness definitions represented in Figure 4.

To design a particular rubber bushing, the stiffness in certain direction needs to meet the requirements. The aim of

this study is to make the radial, axial, and torsional stiffness characteristics of the proposed rubber bushing model meet the target stiffness curves by using the optimization method presented in this study.

It can be noted in the above characteristic curves that there are different requirements in the radial, axial, and torsional directions, such that the objective of the optimization is not limited to a single characteristic. Although it is a complex process to optimize rubber bushings, a good design must satisfy all the characteristics.

**4.2. Data and Information Collection.** Determination of the stiffness in an automotive bushing is often necessary in order to ensure that excessive forces or deflections do not occur [13]. To determine this quantity theoretically, it is necessary to solve the elastic problem in which a cylindrical annulus of



finite length is deformed by means of a relative motion of its curved surfaces, while its initially plane ends remain free from applied forces [20].

Standard textbooks provide some formulas, but they use simpler and approximate relations. Determination of the relevant stiffness is calculated by finite element analysis, using truncated Fourier and Bessel functions or through principal mode approaches [21]. The next formulas have been considered for this study with the theoretical consideration that it is assumed throughout that the rubber is homogeneous, isotropic, and incompressible and that the displacement gradients are sufficiently small for the classical linear theory of elasticity to be applicable.

**4.2.1. Torsional Stiffness.** When the outer cylinder is rotated about its axis with respect to the inner cylinder, the rubber tube between them is subjected to a torsional shearing deformation [13]. According to equation (2), a general equation for torsional stiffness was developed by Adkins and Gent [20] based on a cylindrical rubber bushing of length  $L$  with inner and outer radii  $a$  and  $b$  (Figure 5) and elastic shear modulus  $\mu$ :

$$K_T = \frac{M}{\phi} = \frac{4\pi a^2 b^2 L}{b^2 - a^2} \mu. \quad (12)$$

**4.2.2. Radial Stiffness.** The radial mode is defined as a translation of one sleeve relative to the other sleeve in which each point moves an equal distance perpendicular to the centerline [22].

$$\mathcal{D} \dots = \frac{4(b^2 + a^2) - ab(b^2 + 3a^2)[I_1(ab)K_0(\alpha a) + I_0(\alpha a)K_1(ab)] - \alpha a(3b^2 + a^2)[I_1(\alpha a)K_0(ab) + I_0(ab)K_1(\alpha a)]}{\alpha^2 ba(b^2 + a^2)[I_1(ab)K_1(\alpha a) - I_1(\alpha a)K_1(ab)]}, \quad (14)$$

where  $I_n(ar)$  and  $K_n(ar)$  are the modified Bessel functions for the first and second kind of order  $n$ ,  $r$  is the radius, and  $\alpha^2 = (60/L^2)$ , depending on the length of the bushing.

**4.2.3. Axial Stiffness.** The behavior of hollow rubber tubes under small shear deformations is similar to that of rubber blocks. When the inner cylinder is displaced a distance about its own axis then is subjected to a simple shear deformation. When the length  $L$  is long compared to the wall thickness  $(b - a)$  (Figure 5), the axial stiffness can be obtained by [20]

$$K_A = \mu Q_1 L, \quad (15)$$

where

$$Q_1 = \frac{2\pi}{\log(b/a)}. \quad (16)$$

When the length  $L$  is small compared with the annular distance  $(b - a)$ , the mounting may be regarded as a circular

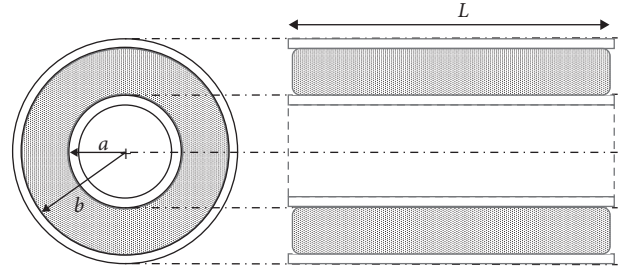


FIGURE 5: Nomenclature used for the static stiffness formulas where  $a$  represents the inner radius,  $b$  represents the outer radius, and  $L$  represents the length of the cylinder.

In the literature review related to the radial stiffness, some interesting results have been obtained. For instance, in the study of Hill [23], an expression for the reduced radial stiffness in terms of infinite Fourier and Fourier-Bessel series was derived, but numerical evaluations are complex. For special cases, Hill [23] proposed a particular formula for the reduced radial stiffness of long and short bushes. Then, Horton [24], based on the classical theory of elasticity, derived a clearer and exact representation for the radial stiffness, in terms of modified Bessel functions, using the principle of superposition for two loading situations. According to Horton [24], the required stiffness of a bushing of length  $L$  with inner and outer radii  $a$  and  $b$  (Figure 5) is given by

$$K_R = \frac{10\pi\mu L}{(7/2)\ln(b/a) - (3/2)(b^2 - a^2/b^2 + a^2) + \mathcal{D}}, \quad (13)$$

where

disk and the relations between force and deflection obtained for small displacements by employing the classical theory for the bending of elastic plates [20]:

$$K_A = \frac{\mu Q_2 L^3}{b^2}, \quad (17)$$

where

$$Q_2 = \frac{16\pi X^2 (X^2 - 1)}{3[(X^2 - 1)^2 - 4X^2 (\log X)^2]}, \quad (18)$$

$$X = \frac{b}{a}.$$

For bushings of moderate length, neither of the assumptions of equations (15) and (17) are adequate, such that an approximation can be used to estimate the stiffness in axial deflection by regarding the resultant displacement of the inner cylinder as the sum of separate displacements due to shearing and bending, respectively, of the elastic material, resulting in the following:

$$K_A = \frac{\mu L}{(1/Q_1) + (b^2/L^2 Q_2)}. \quad (19)$$

**4.3. Validation of the Stiffness Formulation.** Before using the aforementioned axial, radial, and torsional stiffness formulas as our mathematical formulation in the multiobjective optimization problem, this section proves the validity of the formulas and finds how close they are to experimental values reported in the literature.

For this task, the experimental results of Adkins and Gent [20] are considered. In this case, the experimental data were obtained from eight bushings with different lengths but with the same external and internal radius and a single bushing with different internal and external radius. Then, load-deflection measurements were made under torsional, axial, radial, and titling deflection. In this case, we ignored the titling deflection because it is not an objective of this study. For comparison purposes, the reduced values of the stiffness were considered, i.e., the measured stiffness (kg/cm or kg-cm/rad) is divided by the length (cm) of the rubber bushing and by the appropriate value for the rigidity modulus (kg/cm<sup>2</sup>). The reduced stiffness values obtained by the experimental data were compared by the reduced stiffness calculated by equation (12) for the torsional, equation (19) for the axial, and equation (13) for the radial stiffness.

According to the results presented in Figure 6, the three formulas for every mode of deflections present an approach very close to the experimental results. In the radial stiffness curve, there is a discrepancy between the theoretical and experimental data for bushings with length greater than 2.5 cm; this deviation occurs due to the elastomer debonding [10]. Adkins and Gent [20] mention that maximum deflection during the experiments was about 0.1 cm, so in this case, longer bushes would become overstressed. On the contrary, in axial stiffness, we can see the same tendency between theoretical and experimental values, even more accurate in short bushings. By last, in the torsional stiffness, the theoretical values and experimental clearly follow the same tendency with an error of less than 1 percent.

In conclusion, this comparative analysis shows that the use of the corresponding stiffness formulas in the multi-objective optimization problem is adequate for designing an optimal automotive rubber bushing.

**4.4. Definition of Design Variables.** The design variables in an optimization problem denote that variables can influence the result of the objective functions. It is required that before choosing a design variable, there must be an understanding of the physics and the influence of the variable. Selecting the design variables is one of the most important decisions in optimal design.

The design of the component is as simple as possible; thus, the model of the bushing is a representation of a cylindrical rubber material bonded between two steel tubular elements, an outer sleeve of 4 mm thick and an inner sleeve of 5 mm thick. The objective functions are based on the axial, radial and torsional stiffness; therefore, our

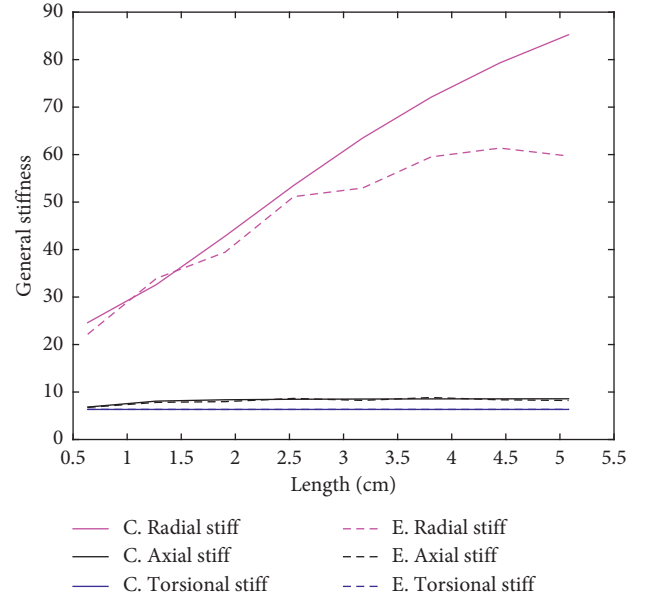


FIGURE 6: A general overview of the accuracy of the calculated theoretical values (C.) versus experimental data (E.).

variables are defined in the parameters that most affect the rubber bushing stiffness characteristics. The optimization of the bushing is given by the geometry of the elastomeric material, specified by length  $L$ , outer radius  $b$ , inner radius  $a$ , and shear modulus  $\mu$ . Varying the values of these four parameters, the geometry of the bushing is modified, and consequently, the stiffness. These four parameters are the design variables of the optimal design problem and can be expressed as four-dimensional vector by

$$x = [a, b, L, \mu]. \quad (20)$$

**4.5. Definition of Objective Function(s).** An objective function must be a scalar function whose numerical value can be obtained once a design is specified and must be a function of the design variable vector  $x$ . Functions need to be maximized or minimized depending on the problem requirements. The selection of a proper objective function is an important decision also in the design process.

In this case, the objective function is considered to minimize the error between the target stiffness curve (given by a dataset) and the theoretical stiffness formulation. However, because the automotive bushing is subject to three deflection modes, three stiffness characteristic curves are used for establishing a multiobjective function. The formulas to obtain the stiffness at each mode, and the requirements were given previously. Since the length, inner radius, outer radius, and shear modulus influence directly the stiffness of the bushing, and considering that a multiobjective problem is often solved by combining its multiple objectives into one single-objective scalar function, a valid general objective function to minimize the difference between the target stiffness and the original stiffness of each partial objective must be defined by

$$F(x) = \sum_{i=1}^3 \left[ \frac{F_i(x) - F_i^*}{F_i^*} \cdot w_i \right], \quad (21)$$

where  $F_i(x)$  represents the formula for axial, radial, and torsional stiffness, respectively,  $F_i^*$  is the target stiffness for each mode obtained by the characteristic curves, and  $w_i$  is the weight of each partial objective. In this simulated environment, the axial stiffness, radial stiffness, and torsional stiffness have the same importance; thus, each  $w_i$  is defined as 1 for each partial objective. The general goal for  $F(x)$  is a four-dimensional vector of  $[0, 0, 0, 0]$ .

**4.6. Formulation of Constraints.** All restrictions placed on the design are collectively called constraints. Results must fit into the available space. The design of a system is a set of numerical values assigned to the design variables. A design meeting all requirements is called a feasible design. An infeasible design does not meet one or more of the requirements.

In this study, the constraints are defined by lower and upper boundaries (implicit constraints) and an inequality constraint. In order to guarantee the feasibility of the optimization, and according to the stiffness formulas, a design space was defined by boundaries where the inner radius  $a$  can be from 6 to 10 mm, the outer radius  $b$  from 10 to 30 mm, the length  $L$  from 60 to 100 mm, and a shear modulus  $\mu$  from 0.5 to 1.5 MPa. These implicit constraints can be expressed also as two four-dimensional vectors given by

$$\begin{aligned} lb &= [5, 10, 60, 0.5], \\ ub &= [10, 30, 100, 1.5]. \end{aligned} \quad (22)$$

Most design problems have inequality constraints. Note that the feasible region with respect to an inequality constraint ( $c(x) \leq 0$ ) is much larger than that with respect to the same constraint expressed as equality ( $ceq(x) = 0$ ). For this study, a simple inequality constraint is given by  $a < b$  because the inner radius cannot be larger than the outer and is written as

$$c(x) = a - b. \quad (23)$$

## 5. Optimization Analysis: Solution Algorithm

The complexity of the optimization of an automotive bushing is due to the large number of different requirements which are in conflict with each other in order to meet the design goals. For this, it is a challenge for engineers to design efficient and cost-effective systems without compromising their integrity. In Figure 7, a proposed flow chart about the optimum design method for an automotive rubber bushing is presented, note also in the flow chart how the iterative algorithm works to optimize the parameters.

In this case, the considered optimum design method has three main blocks: *problem definition*, *multiobjective optimization*, and *validation*. In the *problem definition* block starts the optimization method; basically, here the problem is formulated in variables, constraints, and objectives (such as in Section 4). Then, the initial parameters are introduced defining an initial design model considered as the start point in the optimization procedure.

The *multiobjective optimization* block corresponds essentially to the used goal attainment algorithm. Firstly, an analysis of the system is performed to compute the best model to represent the axial, radial, and torsional stiffness of the current design (local optimization), considering the known set of parameters. Then, the design method checks for satisfaction of all the constraints and determines if the multiobjectives track the defined targets. If the stopping criteria is not fulfilled (multitracking error), the sequential quadratic programming method performs to find the best global optimization design that subsequently is analyzed in local way to check again the constraints. This iterative procedure is stopped if the specified stopping criteria are met, in this case if the axial, radial, and torsional stiffness targets are achieved with an assumed error tolerance.

Finally, the validation block is used to validate the obtained optimal rubber bushing design. In this case, an FEA-based simulation is considered whose inputs correspond to the design parameters resulting from the optimization algorithm. If the optimized model meets simulation results, the validation is done, and it can be considered high percentage of confidence.

This optimization problem formulated in the previous section was solved by using the proposed methodology based in a goal attainment method. The resultant mathematical model of the problem formulation was imported in the MATLAB® software, and the optimization was run. After different starting values, an initial design is estimated and optimizations converged to the same point. Results are shown in Table 1.

**5.1. Validation of the Technical Feasibility.** Usually after a product design, even more for an optimal design, it is necessary to prove its feasibility (technical and economical mainly) [27]. Indeed, product design changes frequently through the design stages, while the optimal design is supported by any engineering analysis (static or dynamic). In this case, for the technical feasibility analysis, the ideal scenario is the manufacturing of the rubber bushing with the optimal parameters reported in Table 1, then making the experimentation and checking with experimental data if the radial, axial and torsional stiffness achieve the desired targets. In the absence of an experimental platform, an FEA-based simulation was considered in this paper. A parametric CAD of a bushing was designed and loaded in the finite element commercial software. The input parameters in the FEA-based simulation are mainly the model structural parameters reported in Table 1. For a comparative study, firstly, the proposed initial design values were used and subsequently the optimal values obtained by the multiobjective optimization problem.

In the modern times, the FEA has become established as the universally accepted analysis method in structural design. The method leads to the construction of a discrete system of a matrix equation to represent the mass and stiffness effects of a continuous structure [25]. As indicated above, firstly, an FEA is established using the proposed initial design and then using the optimized design parameters; for instance, Figure 8 shows the final mesh of the



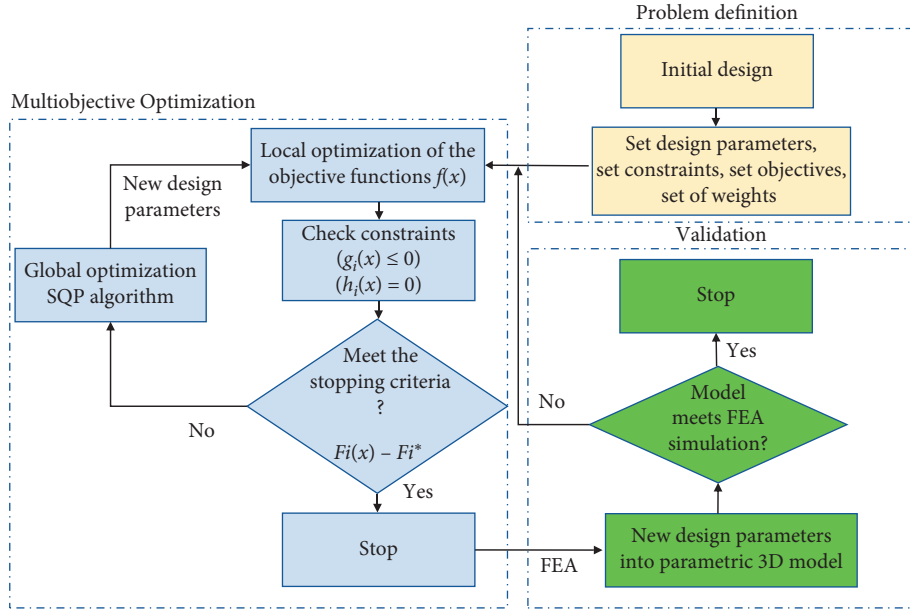


FIGURE 7: Proposed optimization methodology.

TABLE 1: Proposed model structural parameter values and optimal values given by the optimization in MATLAB®.

	Design variables		
	Proposed	Optimized	
Inner radius	10 mm	11.8902	11.9 mm
Outer radius	25 mm	23.8979	23.9 mm
Length	60 mm	64.9193	65 mm
Shear modulus	1 MPa	1.1214	1.1 MPa



FIGURE 8: Final mesh for the 3D model of the automotive bushing.

optimized model. It is well known that a fine mesh gives more accurate simulation results than a coarse mesh. In this study, the bushing was characterized by a fine mesh because the overall assembly geometry increases the number of

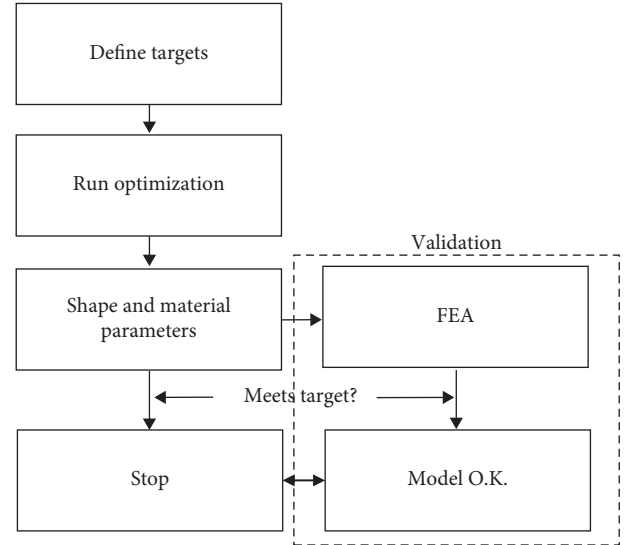


FIGURE 9: Block diagram of the validation procedure using FEA-based simulation.

elements required to ensure the model stability in this application. The final mesh was solid mesh type with around 76186 nodes and 52015 total elements.

The inner and outer sleeves of the elastomeric material were defined as rigid elements by a constraint, with the aim of simulating the presence of the steel surfaces. The contact between the bodies is defined as bonded; indeed, the whole assembly is assumed as global bonded by default. Bonding allows all components touching each other to act as one; thus, thanks to that the inner sleeve is fixed to avoid any movement (cylindrical faces have 3 rotational movements and 3 translational movements), the movements of the elastomer material and outer sleeve are also limited. In the real application, the inner sleeve is fixed by a bolt, and the

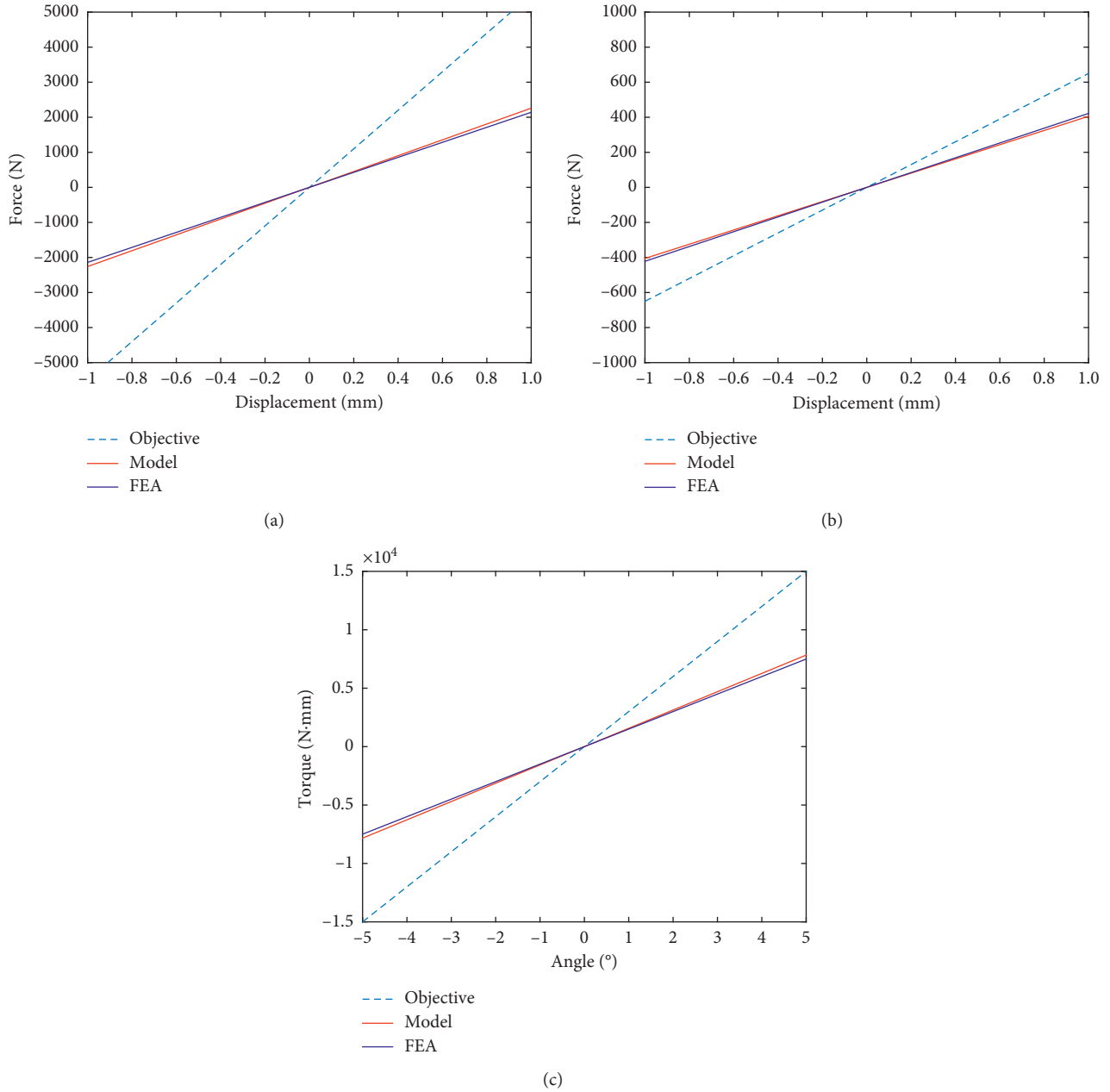


FIGURE 10: Stiffness requirements, mathematical model, and finite element method of the initial proposed model. (a) Radial stiffness proposed model comparison. (b) Axial stiffness proposed model comparison. (c) Torsional stiffness proposed model comparison.

loads are applied on the outer sleeve, so the same environment was simulated. Finally, the isotropic solid was modeled as a hyperelastic material using the Mooney–Rivlin model with constants  $C_{10}$ ,  $C_{01}$ , and  $D_1$ . Mooney–Rivlin models are very common to model large strain nonlinear behavior because they work well for moderately large strains. For this validation, the three constants were obtained from experimental results and modeling using the original first-order Mooney–Rivlin equation from the literature [29, 30].

There are three deflection modes for an automotive bushing, so in the simulations in this study, three different sets for each deflection mode were performed. Although the material, the contacts between components, and the

constraints are the same, the applied force is different in each case. The displacement in the radial, axial, and torsional mode was analyzed in order to determine stiffness in each mode given by the FEA-based simulation and compare it with the mathematically optimized model. Figure 9 illustrates a block diagram of the considered validation procedure, using an FEA-based simulation environment. Note in Figure 9 that the bushing design parameters obtained by the multiobjective optimization algorithm are inputs in the FEA-based simulation, such that the bushing dynamic behavior can be studied by the simulation tests. For the same study but in an experimental platform, these optimal parameters would be input data in the manufacturing phase of

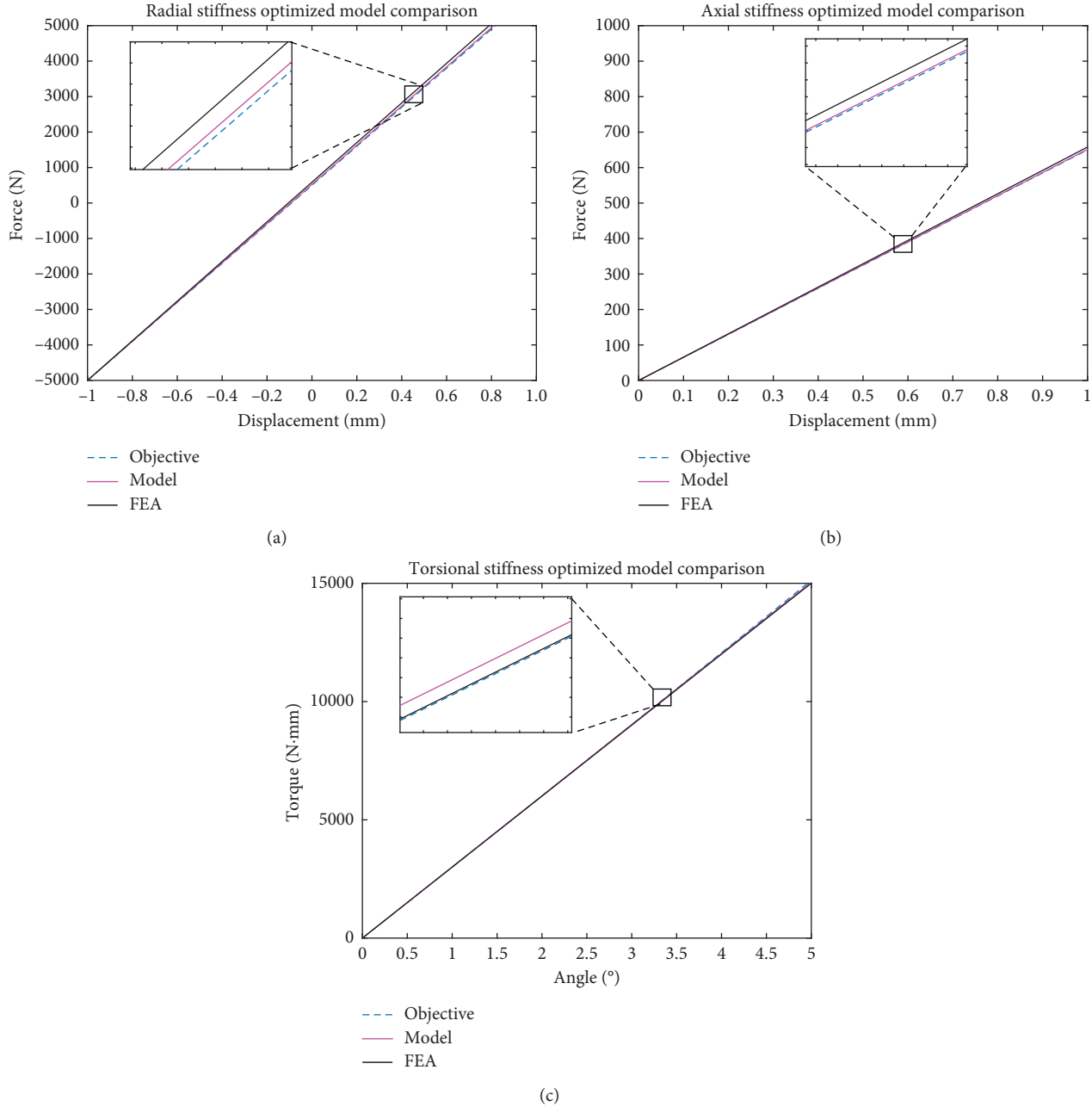


FIGURE 11: Stiffness requirements, mathematical model, and finite element method of the optimized model. (a) Radial stiffness optimized model comparison. (b) Axial stiffness optimized model comparison. (c) Torsional stiffness optimized model comparison.

the bushing. Then, the results obtained by this optimal design (considering an experimental prototype or a proper simulation) must track the specified targets that can be provided by customer requirements.

## 6. Results

The results are structured in stages. The first stage compares the resultant stiffness of the proposed initial design with the requirements. The second stage compares the optimized model results with the stiffness targets. In general, the stiffness of a part is defined as the amount of force required to cause a unit of deflection. To represent the stiffness given

by the FEA, for each mode of deflection, a unit of force was applied and divided by the resultant displacement in the direction of the applied force (radial and axial) and for the inverse tangent of the displacement divided by the radius of the cylinder (torsional).

**6.1. Initial Design.** We proposed a model to meet the stiffness requirements based on intuition comparing sizes and various models of commercial bushings. The proposed 3D model geometry (Table 1) was introduced in the mathematical model to calculate the stiffness using the analytic formulation. The same data provided from the

initial design were loaded in the finite element software, and an analysis was carried out.

Figure 10 illustrates the comparative results in terms of the stiffness requirements for the application. Note in Figure 10 (three cases) that the proposed design does not meet the requirements, and the reason is that it is very difficult to make an intuitive design even when the designer has experience without knowing the environment of each of the design variables.

**6.2. Optimized Design.** In the second stage, the problem was formulated as an optimization problem, and using a mathematical model and through a goal attainment algorithm, the four design variables were optimized. These results were introduced in the mathematical model to calculate the stiffness using the analytic formulation. Likewise, the 3D parametric model was modified with the optimal parameters and loaded into the finite element software for analysis. The results were compared in MATLAB® with the initial stiffness requirements.

Figure 11 shows that, for the three deflection modes (axial, radial, and torsional), the stiffnesses obtained by the FEA-based simulation track very well the mathematical model formulations, considering the optimal parameters of design. In this sense, the optimal parameters of Table 1 obtained by the goal attainment algorithm are the best ones to track the multitargets defined in Figure 4. The differences among the targets, the optimized mathematical model, and the FEA-based simulation (considered as highly complex structural model that substitutes an experimental validation) are minimal. The amplified graphs show that the differences among the curves are small biases, practically negligible.

Consequently, these FEA-based simulations validate the proposed multiobjective optimization problem as a methodology to achieve an optimal design for an automotive rubber bushing.

## 7. Conclusions

This study focused on developing and validating a mathematical model using a numerical algorithm that simplifies the optimization for an automotive rubber bushing to meet specific stiffness characteristics.

The model presented in this study, using a multi-objective function based on a goal attainment method algorithm, was able to reach three different requirements with four variables. In order to validate the results of optimization using the mathematical model, simulations were carried out using the finite element software. Results of the estimated stiffness between the mathematical model and FEA-based simulation were compared. Both curves show qualitatively high coincidence with respect to the same targets; quantitatively, the error in both cases (mathematical model and finite element method of the optimized model) is less than 5%. However, for finite element simulations, the analyzes took hours and high computational cost, while the mathematical model only required minutes without special computational resources.

The proposed mathematical model can streamline the conventional design process for a rubber bushing and decrease trial and error attempts. Even the model allows the design costs and time to be exponentially reduced since it is not necessary to use the software of finite elements because the approximation by the mathematical model is less than five percent of error and can be controlled.

One of the implicit objectives when optimizing the design process of a bushing is to be able to realize rapid prototypes to test new materials and technology, new geometries and sizes, and reduce stress, weight, or volume. Finally, the model can be considered feasible and with a high confidence level for good approximations in complete models of the entire vehicle.

## Data Availability

All data used to support the findings of this study are available from the corresponding author upon request.

## Conflicts of Interest

The authors declare that they have no potential conflicts of interest with respect to the research, authorship, and/or publication of this article.

## Acknowledgments

The authors thank Universidad de Monterrey and Università degli Studi di Modena e Reggio Emilia for their partial financial support to this research project.

## References

- [1] B. HeiBing and M. Ersoy, *Chassis Handbook: Fundamentals, Driving Dynamics, Components, Mechatronics, Perspectives*, Springer Science & Business Media, Berlin, Germany, 2010.
- [2] N. Kaya, "Shape optimization of rubber bushing using differential evolution algorithm," *The Scientific World Journal*, vol. 2014, Article ID 379196, 9 pages, 2014.
- [3] T. Techasen, K. Wansasueb, N. Panagant, N. Pholdee, and S. Bureerat, "Multiobjective simultaneous topology, shape and sizing optimization of trusses using evolutionary optimizers," *IOP Conference Series: Materials Science and Engineering*, vol. 370, no. 1, article 012029, 2018.
- [4] M. Kaldas, K. Çalışkan, R. Henze, and F. Küçükay, "Optimization of damper top mount characteristics to improve vehicle ride comfort and harshness," *Shock and Vibration*, vol. 2014, Article ID 248129, 15 pages, 2014.
- [5] Q. Li, X. Yu, and J. Wu, "An improved genetic algorithm to optimize spatial locations for double-wishbone type suspension system with time delay," *Mathematical Problems in Engineering*, vol. 2018, Article ID 6583908, 8 pages, 2018.
- [6] A. C. Mitra, T. Soni, and G. R. Kiranchand, "Optimization of automotive suspension system by design of experiments: a nonderivative method," *Advances in Acoustics and Vibration*, vol. 2016, Article ID 3259026, 10 pages, 2016.
- [7] S. T. Zhou, Y. J. Chiu, and I. Lin, "The parameters optimizing design of double suspension arm torsion bar in the electric sight-seeing car by random vibration analyzing method," *Shock and Vibration*, vol. 2017, Article ID 8153756, 9 pages, 2017.



- [8] H. Pang, H. Y. Li, Z. D. Fang, and J. F. Wang, "Stiffness matching and ride comfort optimization of heavy vehicle's suspension based on ADAMS," *Applied Mechanics and Materials*, vol. 44, pp. 1734–1738, 2011.
- [9] X. Xu, C. Su, P. Dong, Y. Liu, and S. Wang, "Optimization design of powertrain mounting system considering vibration analysis of multi-excitation," *Advances in Mechanical Engineering*, vol. 10, no. 9, article 1687814018788246, 2018.
- [10] R. Tikani, N. Vahdati, and S. Ziaei-Rad, "Two-mode operation engine mount design for automotive applications," *Shock and Vibration*, vol. 19, no. 6, pp. 1267–1280, 2012.
- [11] D. Özcan, Ü. Sönmez, and L. Güvenç, "Optimisation of the nonlinear suspension characteristics of a light commercial vehicle," *International Journal of Vehicular Technology*, vol. 2013, Article ID 562424, 16 pages, 2013.
- [12] J. Kadlowec, A. Wineman, and G. Hulbert, "Elastomer bushing response: experiments and finite element modeling," *Acta Mechanica*, vol. 163, no. 1, pp. 25–38, 2003.
- [13] A. N. Gent, *Engineering with Rubber: How to Design Rubber Components*, Carl Hanser Verlag GmbH Co KG, Munich, Germany, 2012.
- [14] J. Arora, *Introduction to Optimum Design*, Academic Press, Cambridge, MA, USA, 2004.
- [15] J. Agnarsson, M. Sunde, and I. Ermilova, *Parallel optimization in MATLAB. Project in Computational Science Report*, 2013.
- [16] A. L. Jaimes, S. Z. Martinez, and C. A. C. Coello, "An introduction to multiobjective optimization techniques," *Optimization in Polymer Processing*, pp. 29–57, 2009.
- [17] MathWorks Global Optimization Toolbox User's Guide, *MATLAB Global Optimization Toolbox User's Guide*, 2012.
- [18] G. Lei, Q. Chen, Y. Liu, and J. Jiang, "An inverse method to reconstruct complete stiffness information of rubber bushing," *Advances in Materials Science and Engineering*, vol. 2013, Article ID 187636, 6 pages, 2013.
- [19] G. Previati, M. Kaliske, M. Gobbi, and G. Mastinu, "Structural optimization of a rubber bushing for automotive suspension," in *Proceedings of the 7th European Conference on Constitutive Models for Rubber, ECCMR VII*, pp. 307–312, Dublin, Ireland, September 2011.
- [20] J. E. Adkins and A. N. Gent, "Load-deflexion relations of rubber bush mountings," *British Journal of Applied Physics*, vol. 5, no. 10, pp. 354–358, 1954.
- [21] M. J. García Tárrago, L. Kari, J. Viñolas, and N. Gil-Negrete, "Torsion stiffness of a rubber bushing: a simple engineering design formula including the amplitude dependence," *Journal of Strain Analysis for Engineering Design*, vol. 42, no. 1, pp. 13–21, 2007.
- [22] K. Hasanpour, S. Ziaei-Rad, and M. Mahzoon, "A large deformation framework for compressible viscoelastic materials: Constitutive equations and finite element implementation," *International Journal of Plasticity*, vol. 25, no. 6, pp. 1154–1176, 2009.
- [23] J. M. Hill, "Radical deflections of rubber bush mountings of finite lengths," *International Journal of Engineering Science*, vol. 13, no. 4, pp. 407–422, 1975.
- [24] J. M. Horton, M. J. C. Gover, and G. E. Topholme, "Stiffness of rubber bush mountings subjected to radial loading," *Rubber Chemistry and Technology*, vol. 73, no. 2, pp. 253–264, 2000.
- [25] M. Friswell and J. E. Mottershead, *Finite Element Model Updating in Structural Dynamics*, Vol. 38, Springer Science & Business Media, Berlin, Germany, 2013.
- [26] Z. Liu, S. Yuan, S. Xiao, S. Du, Y. Zhang, and C. Lu, "Full vehicle vibration and noise analysis based on substructure power flow," *Shock and Vibration*, vol. 2017, Article ID 8725346, 17 pages, 2017.
- [27] W. Wei, A. Liu, A. Liu, S. C.-Y. Lu, and T. Wuest, "Product requirement modeling and optimization method based on product configuration design," *Procedia CIRP*, vol. 36, pp. 1–5, 2015.
- [28] J. Ambrósio and P. Verissimo, "Sensitivity of a vehicle ride to the suspension bushing characteristics," *Journal of Mechanical Science and Technology*, vol. 23, no. 4, pp. 1075–1082, 2009.
- [29] D. F. Lalo and M. Greco, "Rubber bushing hyperelastic behavior based on shore hardness and uniaxial extension," in *Proceedings of the 24th ABCM International Congress of Mechanical Engineering, COBEM-2017-5280*, Curitiba, Brazil, December 2017.
- [30] B. Bscheiden, B. Ferguson, and D. Sameoto, "Hyperelastic simulation for accurate prediction of gecko inspired dry adhesive deformed shape and stress distribution prior to detachment," in *Proceedings of the Annual Meeting of the Adhesion Society*, Daytona Beach, FL, USA, March 2013.

